Available online at www.sciencedirect.com
SCIENCE DIRECT®
Journal of Sound and Vibration 289 (2006) 509–528
JOURNAL OF SOUND AND VIBRATION
www.elsevier.com/locate/jsvi

Equivalent constitutive model-based design of wave-absorbing material system and controller

D. Roy Mahapatra*

Department of Aerospace Engineering, Indian Institute of Science, Bangalore 560012, India

Received 23 March 2004; received in revised form 10 January 2005; accepted 14 February 2005
Available online 20 April 2005

Abstract

A design methodology for wave-absorbing active material system is reported. The design enforces equivalence between an assumed material model having wave-absorbing behavior and a set of target feedback controllers for an array of microelectro-mechanical transducers which are integral part of the active material system. The proposed methodology is applicable to problems involving the control of acoustic waves in passive–active material system with complex constitutive behavior at different length-scales. A stress relaxation type one-dimensional constitutive model involving viscous damping mechanism is considered, which shows asymmetric wave dispersion characteristics about the half-line. The acoustic power flow and asymptotic stability of such material system are studied. A single sensor non-collocated linear feedback control system in a one-dimensional finite waveguide, which is a representative volume element in an active material system, is considered. Equivalence between the exact dynamic equilibrium of these two systems is imposed. It results in the solution space of the design variables, namely the equivalent damping coefficient, the wavelength(s) to be controlled and the location of the sensor. The characteristics of the controller transfer functions and their pole-placement problem are studied.

1. Introduction

Control of traveling waves in structures have been studied extensively by various authors [1–7]. This is one of the important areas of development in distributed parameter active/passive control

*Tel.: +91 080 22932438; fax: +91 080 23600134.
E-mail address: dprasad@aero.iisc.ernet.in.

0022-460X/$ - see front matter © 2005 Elsevier Ltd. All rights reserved.
doi:10.1016/j.jsv.2005.02.011

system for high-performance adaptive structures. Typical applications of this wave control problem are the control of structure-borne vibration and noise, disturbance rejection in high-speed flexible manipulators, precision broadband control of pointing devices, space systems in microgravity environment, etc.

Structural wave control problem leads to the Low Authority Control (LAC) problem [8,9] as opposed to the High Authority Control (HAC) problem, the latter being concerned with the steady-state vibration. This is of particular significance in developing *auxiliary* control system for disturbance rejection in large space structures, where the controller natural frequencies must lie far above several structural natural frequencies [10]. Although the HAC problem is generally analyzed using modal method in second-order form or state-space method in first-order form, both the HAC as well as LAC problems can be treated efficiently using harmonic wave approach [3,11,12]. In harmonic wave approach for designing wave controller, most of the models developed till date are either based on wave cancellation [1,4,13] or based on minimization of frequency domain cost over prescribed frequency band [14–16]. Stability in collocated LAC can be ensured by providing a compensator which is strictly positive real [5,17,18]. But, in non-collocated LAC and HAC, it is essential to identify the bound on the non-collocated configuration defined by the sensor–actuator locations, feedback gains, etc. A method for optimal gain selection based on Lyapunov's direct method and wave equation in Laplace domain was proposed by Alli and Singh [5]. They obtained the bounds on the gain parameters by studying the root-locus for collocated and non-collocated configuration. Although such analytical approach ensures the stability of the closed-loop MIMO system by boundary control, its application for disturbance rejection in complex skeletal structures appears numerically intensive. Currently there are two major difficulties toward the development of wave-absorbing controller based on wave cancellation approach, especially for non-collocated configuration. One is the energy required for perfect cancellation of individual wave modes. It has been reported by Gardonio and Elliott [15] that cancellation of any one of the propagating wave modes in a rod/beam creates additional secondary waves at the scattering termination. Similar effect has also been reported by Roy Mahapatra et al. [12] while studying the dynamics of single-actuator-multiple-waves. Understanding of the bounded energy input for partial cancellation of the wave modes remains an open area of research. The second difficulty is the instability due to the synchronization error in wave cancellation, which is more likely to occur at higher frequencies.This is due to the high-frequency limitation of the controller [2,19]. The acoustic limit of the controller is posed by the finite time delay, which gets introduced due to the interface electronics and the digital signal processor for a given feedback control algorithm. Non-dispersive waves propagate with constant group speed, whereas dispersive waves in a beam propagate with group speed proportional to the square root of the excitation frequency. Hence, it is essential to introduce appropriate robustness against time delay in the design of the wave-absorbing controller. Related understanding is also not well reported. While implementing the active wave controller, it is generally emphasized that the use of additional passive devices augments the overall performance of the active/passive system. Active/passive Tuned Mass Dampers (TMDs) are typically designed based on this approach, where the high-frequency components are attenuated by the viscoelastic mechanisms, and few low-frequency resonant modes are attenuated actively by the anti-resonance of the TMD dynamics.

Due to tremendous development in materials technologies, there is a wide possibility that the passive damping or wave attenuation properties can be efficiently tailored by controlling the

microstructure of the material. For example, it is possible to augment the passive damping performance by introducing stiffness/inertia modulation [20,21]. Lurie [22] has proposed a geometric method based on characteristic lines to visualize the screening phenomenon, which can be used in the design of rank-one laminated composite to block the wave transmission through certain segment of an one-dimensional waveguide. Taking such concept one-step forward, one can design the material-intrinsic damping parameters for stability and optimal control of the wave transmission through such material system under any unknown disturbance. There is another possibility that given a rod/beam like finite waveguide with conventional homogeneous material properties, one can design microcontrollers with feed-back MEMS sensors and actuators, periodically placed along the waveguide span, to perform the above task. That is to provide the active damping capability, which is equivalent to the intrinsic damping of another microstructure controllable material, and associated stability and robustness. A basic modeling, analysis and design framework is reported in this paper to achieve the above objectives. Similar other active/passive mechanisms for design of LAC can also be easily implemented following the same approach. Also, the approach is readily applicable to complex geometry involving network of waveguides.

2. Material constitutive models with spatio-temporal modulation and dissipation

Consider the longitudinal wave propagation in a one-dimensional waveguide, in which the material constitutive model is governed by either a passive material system with certain spatio-temporal dynamics of the microstructure (called hereafter as passive) or an active system with electro-magnetically controlled state of microstructure (called hereafter as active). The idea of establishing an equivalence between these two systems plays the central role in this paper while developing a methodology for controlling a distributed parameter system in one-dimensional space and time.

2.1. Passive material system

This is a hypothetical case of a rod shown in Fig. 1(a) having microstructured material. Assume that the effective properties of the material can be obtained by homogenizing the appropriate microstructural properties [23,24] in the scale of the smallest wavelength (λ_m). Here λ_m can be treated as the mesoscopic scale. For the one-dimensional shape in macroscale, the effective elastic modulus can be expressed as $(1,1)$ component of the homogenized elastic stiffness tensor

$$\mathbf{Q} = \frac{1}{\lambda_m}\int_0^{\lambda_m} \frac{\partial^2 \mathscr{W}}{\partial \mathbf{F}\,\partial \mathbf{F}}\,\mathrm{d}x, \tag{1}$$

where $\mathscr{W}$ is the strain energy density due to microstructural deformation and other non-mechanical effects. $\mathbf{F}$ is the deformation gradient expressed as

$$\mathbf{F} = \begin{bmatrix} 1+\dfrac{\partial u}{\partial x} & 0 & \dfrac{\partial u}{\partial z} \\ 0 & 1 & 0 \\ \dfrac{\partial w}{\partial x} & 0 & 1 \end{bmatrix}, \tag{2}$$

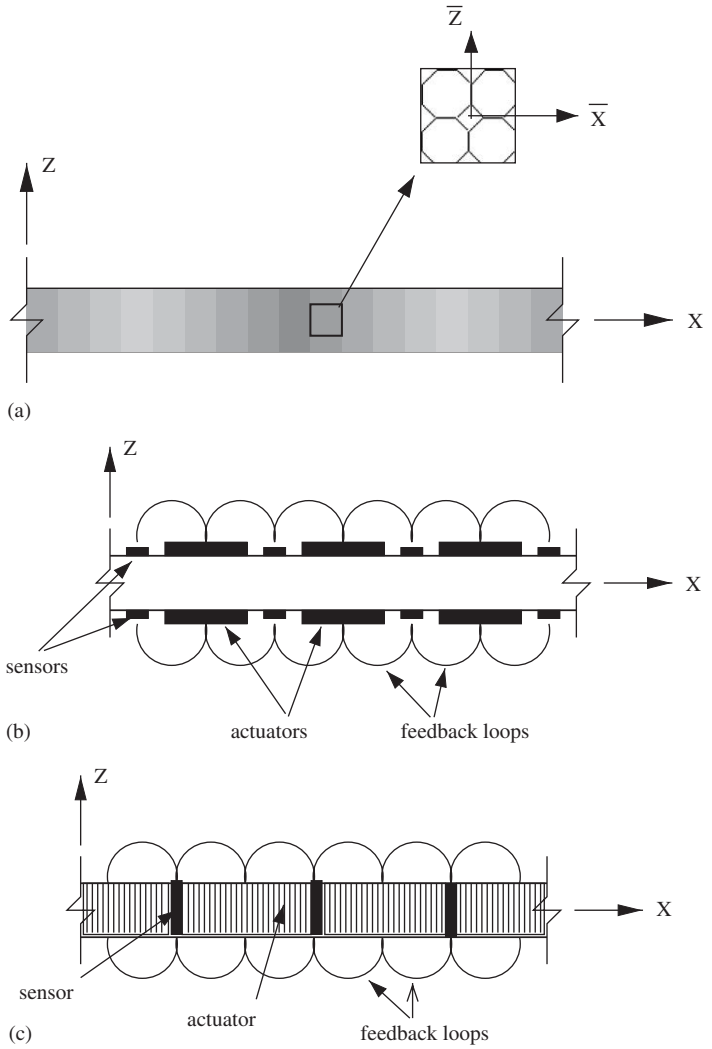

Fig. 1. (a) Rod of microstructured material having viscous dissipation mechanism. (b) Rod with arrays of layered piezoelectric actuators and feedback sensors. (c) Rod with arrays of stacked piezoelectric actuators and feedback sensors.

(u, w) are the longitudinal and transverse displacements defined in the macroscopic coordinate system (x, z) and time t. In order to evaluate Eq. (1), it is necessary to define the energy density $\mathscr{W}$ in terms of the field variables in continuum scale (macroscopic scale) and any additional form of energy functional that takes part in the dynamics where the continuum framework breaks down. The rationale employed later in this paper while developing the control system is that a truly multiscale material system, as realized above, leads to some form of inelastic behavior in the macroscopic scale. In the present problem, the macroscopic scale is the scale in which the proposed control is assumed to be effective. In order to investigate the possible nature of inelastic

behavior arising through a general form of energy functional, we employ the method of multiple scale and obtain the governing equations. This is discussed below. A microscopic scale is first introduced with the coordinate system (x_1, z_1) and slow time (t_1), which are related to the macroscopic scale as

$$x = \varepsilon x_1, \quad z = \varepsilon z_1, \quad t = \varepsilon t_1, \tag{3}$$

where ε is a small parameter associated with the geometry of the microstructure defined next. Let us consider an unit cell in (x_1, z_1) with a dominant phase A of host material in crystalline or cellular network form and another phase B of material as inclusion or void. Let the small parameter ε be the volume fraction of phase B in the unit cell. Then the cell averaged elastic stiffness component (E_1) and the cell averaged mass density (ρ_1) can be defined, respectively, as

$$E_1 = E_A(1-\varepsilon) + \varepsilon E_B, \quad \rho_1 = \rho_A(1-\varepsilon) + \varepsilon \rho_B, \tag{4}$$

where the subscripts A and B, respectively, indicate the material properties of phases A and B. Further, we shall assume $\varepsilon = \varepsilon(x_1, z_1, t_1)$, which is adequate to represent statistical pattern of the microstructure and phase kinetics. For the sake of simplicity while dealing with the one-dimensional case, the kinematics due to transverse motion w is neglected. The longitudinal displacement is expressed as

$$u = u_0(x,t) + \varepsilon u_1(x_1, z_1, t_1), \tag{5}$$

where u_0 and u_1 are the longitudinal displacements defined, respectively, in the macroscopic and the microscopic scales. Using the usual definition of green strain tensor

$$\mathbf{E} = \tfrac{1}{2}(\mathbf{F}^{\mathrm{T}}\mathbf{F} - \mathbf{I}) \tag{6}$$

and following Eq. (2), the longitudinal strain can be written as

$$\varepsilon_{xx} = \frac{\partial u}{\partial x} + \frac{1}{2}\left(\frac{\partial u}{\partial x}\right)^2 + \frac{1}{2}\left(\frac{\partial u}{\partial z}\right)^2. \tag{7}$$

The inelastic part in the energy functional is due to the geometry of the microstructure, electromagnetic polarization of the domains and dynamics of the domain interfaces. Their contribution in the energy functional is assumed here as directly proportional to the volume of phase B, which leads to

$$\mathscr{W} = \int_{\Omega_1} \left(\frac{1}{2} E_1 \varepsilon_{xx} + \varepsilon \mathscr{P}(x_1, z_1, t_1, \cdots)\right) \varepsilon_{xx} \, \mathrm{d}\Omega, \tag{8}$$

where $\mathscr{P}$ is a quasi-linearized force field as a function of the current state of the microstructure. Such a choice of $\mathscr{W}$ eventually leads to the first Piola–Kirchoff stress component

$$\sigma_{xx} = E_1 \varepsilon_{xx} + \varepsilon \mathscr{P} \tag{9}$$

and the equilibrium equation can be expressed as

$$\frac{\partial \sigma_{xx}}{\partial x} = \frac{\partial^2 u}{\partial t^2}. \tag{10}$$

Simplifying Eq. (10) using the two-scale expansion of the displacement given in Eq. (5) and noting the total differentials $\partial \to \partial_0 + (1/\varepsilon)\partial_1$, and then isolating the linear terms according to the order

of ε, we get

$$\mathcal{O}(\varepsilon^{-1}): \quad E_A \frac{\partial^2 u_1}{\partial x_1^2} = \rho_A \frac{\partial^2 u_1}{\partial t_1^2} + (\rho_B - \rho_A)\frac{\partial \varepsilon}{\partial t_1}\left(\frac{\partial u_0}{\partial t} + \frac{\partial u_1}{\partial t_1}\right), \tag{11a}$$

$$\mathcal{O}(1): \quad E_A \frac{\partial^2 u_0}{\partial x^2} + (E_B - E_A + \mathscr{P})\frac{\partial^2 u_1}{\partial x_1^2} + \frac{\partial \mathscr{P}}{\partial x_1}\left(\frac{\partial u_0}{\partial t} + \frac{\partial u_1}{\partial t_1}\right) = \rho_A \frac{\partial^2 u_0}{\partial t^2} + (\rho_B - \rho_A)\frac{\partial^2 u_1}{\partial t_1}, \tag{11b}$$

$$\mathcal{O}(\varepsilon): \quad (E_B - E_A + \mathscr{P})\frac{\partial^2 u_0}{\partial x^2} = (\rho_B - \rho_A)\frac{\partial^2 u_0}{\partial t^2}. \tag{11c}$$

Note that the nonlinear coupled terms have been neglected, the condition $\partial u_1/\partial z_1 = 0$ has been imposed and two additional constraints

$$\frac{\partial \varepsilon}{\partial x_1} = 0, \quad \frac{\partial \varepsilon}{\partial z_1} = 0, \tag{12}$$

obtained by considering the terms above $\mathcal{O}(\varepsilon^{-1})$ have been used. Since we have only two variables u_0 and u_1 and the force field $\mathscr{P}$ is prescribed in quasi-linearized form, therefore only the Eqs. (11a) and (11b) need to be considered, which correspond to higher-order contributions in ε as compared to $\mathcal{O}(\varepsilon)$. It is clear from the coupled system in Eqs. (11a)–(11b) that they represent dispersive and inhomogeneous wave propagation, when $\partial\varepsilon/\partial t_1 \neq 0$, $\partial\mathscr{P}/\partial x_1 \neq 0$. Moreover, if one considers the macroscopic gradation of the microstructure by replacing ε with $\varepsilon'(x)\varepsilon(x_1, z_1, t_1)$ in Eqs. (3)–(5) and following the subsequent steps, where ε' is a specified gradation parameter, then the spatial modulation of the propagation characteristics is obvious. Hence, for rate sensitive and quasi-linearized dynamics of the microstructures with macroscopic gradation, the macroscopic properties can be represented through spatio-temporal modulation of the properties as

$$\mathbf{Q}(x,t) = \mathbf{Q}_0 + \alpha_Q S(x,t), \quad \rho(x,t) = \rho_0 + \alpha_\rho S(x,t), \tag{13}$$

where $\mathbf{Q}_0$ and ρ_0 are, respectively, the rate-independent part of the stiffness and mass density. α_Q, α_ρ are constants. A suitable choice of the spatio-temporal modulation can be

$$S(x,t) = \sin\left(2\pi x/\lambda_m\right)\sin(\omega_m t), \tag{14}$$

where ω_m is the frequency of microstructural oscillation, which is expected to be in the higher side of the frequency band of macroscopic wave propagation. The modulated properties described in Eq. (13) may be employed in designing certain band-pass or band-gap behavior. The combination of rate-dependent and rate-independent properties can be homogenized in the scale of λ_m, but here one needs to consider the momentum balance equations. This aspect can be found in published literature, e.g. [25].

In order to quantify the effect of inelasticity in the passive material system by observing Eqs. (11a)–(11b) into a linearized form of macroscopic constitutive model, a stress relaxation-type

constitutive model

$$\sigma_{xx} = Q_{11}\varepsilon_{xx} - \eta \frac{\partial u}{\partial t} \tag{15}$$

is considered, which is used to design an equivalent controller in this paper. η is a viscous damping coefficient (a rate parameter after homogenization in the mesoscopic scale λ_m).

2.2. Active material system

Since the passive material system discussed in Section 2.1 with a desired spatio-temporal modulation is difficult to manufacture using the present-day technologies, therefore an active equivalent of such system may be considered. One possibility of such active system is an elastic/piezoelectric rod structure (layers/stacks with parametric modulation) and actuation in closed-loop as shown in Fig. 1(b) and (c). In such active system the elastic domain (denoted as $\Omega^{(e)}$) follows the constitutive model $\sigma_{xx}^{(e)} = E_1^{(e)}\varepsilon_{xx}^{(e)}$ and the piezoelectric domain (denoted by $\Omega^{(p)}$) follows the constitutive model $\sigma_{xx} = E_1^{(p)}\varepsilon_{xx} - e_{3j}\mathscr{E}_j, j = 1, 3$, where $\mathscr{E}_j$ is the electric field causing in-plane or transverse polarization of the piezoelectric crystal, e_{ij} are the piezoelectric coefficients. The dynamics of the elastic and the piezoelectric domains can be described, respectively, as

$$\int \frac{\partial}{\partial x}\left(E_1^{(e)}\frac{\partial u^{(e)}}{\partial x}\right)\mathrm{d}z = \int \frac{\partial}{\partial t}\left(\rho^{(e)}\frac{\partial u^{(e)}}{\partial t}\right)\mathrm{d}z, \quad (x,z) \in \Omega^{(e)}, \tag{16a}$$

$$\int \frac{\partial}{\partial x}\left(E_1^{(p)}\frac{\partial u^{(p)}}{\partial x} - e_{3j}\mathscr{E}_j\right)\mathrm{d}z = \int \frac{\partial}{\partial t}\left(\rho^{(p)}\frac{\partial u^{(p)}}{\partial t}\right)\mathrm{d}z, \quad (x,z) \in \Omega^{(p)} \tag{16b}$$

with the kinematics and equilibrium of the interfaces at $\Gamma(x_k, z_k)$ given by

$$u^{(e)} = u^{(p)}, \quad (x,z) \in \Gamma(x_k, z_k), \tag{17a}$$

$$\int E_1^{(e)}\frac{\partial u^{(e)}}{\partial x}\,\mathrm{d}z + \int\left(E_1^{(p)}\frac{\partial u^{(p)}}{\partial x} - e_{3j}\mathscr{E}_j\right)\mathrm{d}z = 0, \quad (x,z) \in \Gamma(x_k, z_k). \tag{17b}$$

Note that both the wave equations (Eqs. (16a)–(16b)) have second-order characteristics, and hence there are two wave modes in both the domains, one is forward propagating and the other is backward propagating. Therefore, considering a single harmonics and by denoting the forward propagating wave as u^+ and the backward propagating wave as u^-, we have

$$u^{(p)} = u^{(p)^+} + u^{(p)^-} \tag{18a}$$

and with the help of interface conditions in Eqs. (17a)–(17b) evaluated over a periodic or aperiodic volume elements, there exists the following linear dependence between the displacement field of the elastic and the piezoelectric domains

$$u^{(e)} = \beta^+ u^{(p)^+} + \beta^- u^{(p)^-}, \tag{18b}$$

$$\beta^+ = \beta^- = 1, \quad (x,z) \in \Gamma(x_k, z_k), \tag{18b}$$

where β^+ and β^- are the functions of the material and geometric properties of the neighboring piezoelectric domain. If velocity feedback is chosen for prescribing the electric field, then

$$\mathscr{E} = \gamma \frac{\partial u}{\partial t}, \quad u \in \{u^{(e)}, u^{(p)}\}, \tag{19}$$

where γ is a feedback gain parameter. Now, an equivalence can be observed between the passive and the active system through the relationship between the rate parameter η defined in Eq. (15) with the feedback gain parameter γ as $\eta = \eta(Q_{ij}, e_{ij}, \gamma)$, where the dynamics of a representative volume element with homogenized properties of the active system can be expressed as

$$I_0 \frac{\partial^2 u}{\partial t^2} - A_{11} \frac{\partial^2 u}{\partial x^2} + \eta A \frac{\partial^2 u}{\partial x \partial t} = 0, \quad (x, z) \in \Omega^{(e)} \cup \Omega^{(p)} \tag{20}$$

and the applied boundary conditions at $x = 0, L$ are

$$u = u(0, t), u(L, t) \quad \text{or} \quad A_{11} \frac{\partial u}{\partial x} - \frac{1}{2} \eta A \frac{\partial u}{\partial t} = f(0, t), f(L, t), \tag{21}$$

where $I_0 = \int \rho \, \mathrm{d}z$, A is the cross-sectional area, $A_{11} = \int Q_{11} \, \mathrm{d}z$ and $f(x, t)$ is the longitudinal force. The objective is now to design the parameter γ as a function of the prescribed η, and the associated controller characteristics.

If the spatio-temporal modulation of the passive system properties described by Eq. (13) is included, then it can be shown by comparing the corresponding governing equations and the boundary conditions with Eqs. (20)–(21) that

$$\frac{3}{2} \eta A \frac{\partial^2 u}{\partial x \, \partial t} = \alpha_\rho S(x, t) \frac{\partial^2 u}{\partial t^2}. \tag{22}$$

In this manner, an equivalence between the wave screening property of the passive system (through the function $S(x, t)$) and the design variable γ for the active system can be established. This condition is equivalent to generating microactuator force proportional to the strain rate, which is equal to the passive force due to the modulated inertia ($\alpha_\rho S(x, t)$) in the microstructured material. Next, a methodology is described to design the controller for the active system having the above equivalence with the passive system. Characteristics of the modified wave dispersion is studied first.

3. Wave dispersion

Consider an excitation involving multiple harmonics. By applying the Discrete Fourier Transformation (DFT) of the displacement field, one can write

$$u(x, t) = \sum_{n=1}^{N} \hat{u}(x, \omega_n) \mathrm{e}^{\mathrm{i}\omega_n t} = \sum_{n=1}^{N} (\tilde{u}^+ \mathrm{e}^{-\mathrm{i}k_1 x} + \tilde{u}^- \mathrm{e}^{-\mathrm{i}k_2 x}) \mathrm{e}^{\mathrm{i}\omega_n t}, \tag{23}$$

where $\mathrm{i} = \sqrt{-1}$, ω_n is the nth sampling frequency, N is the Nyquist frequency, $\hat{u}$ is the frequency amplitude of the displacement, $\tilde{u}^+$ and $\tilde{u}^-$ are the boundary-dependent wave coefficients associated with, respectively, the forward and the backward propagating waves. k_1 and k_2 are the wavenumbers. Similarly, the dynamic force is transformed into its frequency domain counterpart

(denoted by overhead hat) as

$$f(x,t)=\sum_{n=1}^{N}\hat{f}(x,\omega_n)\mathrm{e}^{\mathrm{i}\omega_n t}. \tag{24}$$

Substituting Eq. (23) in Eq. (20), the dispersion relation is obtained, whose roots are the wavenumbers

$$k_{1,2}=\omega_n\left[-\frac{\eta A}{2A_{11}}\pm\sqrt{\frac{I_0}{A_{11}}+\left(\frac{\eta A}{2A_{11}}\right)^2}\right]. \tag{25}$$

As outlined earlier, the objective here is to embed the above propagation characteristics of a dissipative material system into the control system to be designed for the active rod, which is otherwise undamped with wavenumbers $k_0=\omega_n\sqrt{\rho/E_1}$, and we shall call it nominal system. For the purpose of design, a bound on the damping coefficient η is introduced, which is given by

$$\left(\frac{\eta A}{2A_{11}}\right)^2=\alpha\frac{\rho}{E_1},\quad 0\leqslant\alpha\leqslant 10. \tag{26}$$

3.1. Modification of the speed of propagation

Eq. (25) indicates that the propagation is non-dispersive, hence the phase speed (ω/k) is equal to the group speed ($\mathrm{d}\omega/\mathrm{d}k$). The phase speeds of the forward and the backward propagating waves are, respectively, g^+c and g^-c, where $c=\sqrt{E_1/\rho}$ the nominal speed of propagation in the rod and

$$g^+=\sqrt{\alpha}+\sqrt{1+\alpha},\quad g^-=-\sqrt{\alpha}+\sqrt{1+\alpha}. \tag{27}$$

Fig. 2 shows the variations in g^+ and g^-. It can be seen that the speed of the forward propagation increases many times as compared to the speed of the backward propagation. This also means that the symmetry of the wavefronts with respect to the point of incidence of the source disturbance is no longer preserved.

3.2. Wave amplitude modulation

Consider the forward and the backward propagating waves in the active system with incident disturbance $\hat{f}(0,\omega_n)$ at $x=0$. In closed-loop configuration, the wave in the positive x direction ($x>0$) and the wave in the negative x direction ($x<0$) are, respectively,

$$\hat{u}^+=\frac{\mathrm{i}\hat{f}(0,\omega_n)}{A_{11}k_1+\frac{1}{2}\eta A\omega_n}\mathrm{e}^{-\mathrm{i}k_1x},\quad \hat{u}^-=\frac{\mathrm{i}\hat{f}(0,\omega_n)}{A_{11}k_2+\frac{1}{2}\eta A\omega_n}\mathrm{e}^{-\mathrm{i}k_2x}. \tag{28}$$

For both the wave components, the amplitude modulation becomes independent of the frequency and can be expressed as

$$r=\frac{|\hat{u}^+|}{|\hat{u}_0^+|}=\frac{|\hat{u}^-|}{|\hat{u}_0^-|}=\frac{1}{\sqrt{1+\alpha}}, \tag{29}$$

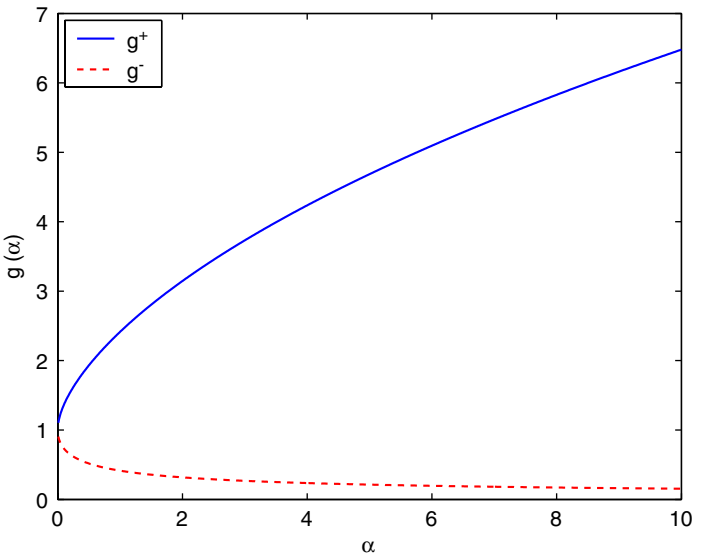

Fig. 2. Variation in the speeds of forward propagation g^+ and backward propagation g^- due to variation in α.

where $\hat{u}_0^+$ and $\hat{u}_0^-$ are, respectively, the forward and the backward propagating waves in the nominal system.

The frequency domain power flow at a given cross-section can be expressed as

$$\hat{P} = \tfrac{1}{2}\hat{f}(\mathrm{i}\omega_n\hat{u})^*, \tag{30}$$

where the superscript $*$ stands for the complex conjugate. The additional power required to provide the control can be estimated as the difference between the power flow in the active system and the power flow in the nominal system (denoted by subscript 0). For the forward wave propagation, this additional power can be derived as

$$\Delta\hat{P}^+ = \hat{P}^+ - \hat{P}_0^+ = \frac{1}{2}\,\omega_n^2\sqrt{A_{11}I_0}\left[1 - \frac{1}{\sqrt{1+\alpha}}\right]\left|\hat{u}_0^+\right|^2 \tag{31}$$

and for the backward wave propagation, this additional power can be derived as

$$\Delta\hat{P}^- = \hat{P}^- - \hat{P}_0^- = \frac{1}{2}\,\omega_n^2\sqrt{A_{11}I_0}\left[1 - \frac{1}{\sqrt{1+\alpha}}\right]\left|\hat{u}_0^-\right|^2. \tag{32}$$

It can be seen from Eqs. (31) and (32) that the input power has bounds, i.e., $0 \leqslant \Delta\hat{P}^+ < \hat{P}_0^+$ and $0 \leqslant \Delta\hat{P}^- < \hat{P}_0^-$, since $0 \leqslant \alpha < \infty$.

3.3. System stability and wave absorbing property

Eqs. (31)–(32) show the boundedness of the compensating system, which can be designed to provide the wave absorbing mechanism in the form of electro-mechanical transduction and heat (in case of the active system) or in the form of microstructural kinetics and heat (if a passive

system becomes realizable). Lyapunov's direct approach can be employed here to study the stability of the system response. Let the Lyapunov functional be

$$V(t) = \frac{1}{2}\int_0^L \int_A \left[\rho\left(\frac{\partial u}{\partial t}\right)^2 + \sigma_{xx}\varepsilon_{xx}\right] \mathrm{d}A\,\mathrm{d}x. \tag{33}$$

Differentiating once with respect to time and expanding in terms of the longitudinal displacement u,

$$\dot{V}(t) = \int_0^L \left[I_0 \frac{\partial u}{\partial t}\frac{\partial^2 u}{\partial t^2} + A_{11}\frac{\partial u}{\partial x}\frac{\partial^2 u}{\partial x \partial t} - \frac{1}{2}\eta A \frac{\partial^2 u}{\partial t^2}\frac{\partial u}{\partial x} - \frac{1}{2}\eta A \frac{\partial u}{\partial t}\frac{\partial^2 u}{\partial x\,\partial t}\right] \mathrm{d}x. \tag{34}$$

Integrating Eq. (34) by parts, and with the help of Eq. (20) and using the following identity:

$$\int_0^L \frac{\partial}{\partial t}\left(\frac{\partial u}{\partial t}\frac{\partial u}{\partial x}\right) \mathrm{d}x = 0, \tag{35}$$

we get

$$\dot{V}(t) = f(L,t)\frac{\partial}{\partial t}u(L,t) - f(0,t)\,\frac{\partial}{\partial t}u(0,t). \tag{36}$$

For every single harmonic wave component (considering either of the forward or the backward propagation separately), $(\frac{1}{2})f(x,t)\dot{u}(x,t)$ is the time domain counterpart of the power defined in Eq. (30). Hence, if the incident wave is applied at $x = 0$ and the assumed damping mechanism is placed at $|x| \geqslant L$, then the frequency domain form of Eq. (36) can be expressed with the help of Eqs. (31) and (32) as

$$\hat{\dot{V}}^+ = -\frac{2}{\sqrt{1+\alpha}}\,\hat{P}(L,\omega_n)_0^+ - 2\hat{P}(0,\omega_n)_0^+ = -2\left[1 + \frac{1}{\sqrt{1+\alpha}}\right]\hat{P}^+ \leqslant 0, \tag{37}$$

$$\hat{\dot{V}}^- = -\frac{2}{\sqrt{1+\alpha}}\,\hat{P}(L,\omega_n)_0^- - 2\hat{P}(0,\omega_n)_0^- = -2\left[1 + \frac{1}{\sqrt{1+\alpha}}\right]\hat{P}^- \leqslant 0, \tag{38}$$

where $\hat{P}_0^+ \geqslant 0$ and $\hat{P}_0^- \geqslant 0$ are, respectively, the forward and the backward flowing powers in the nominal system. It results in negative semi-definiteness of the Lyapunov functional and hence ensures the asymptotic stability of the active system. In other words, $|\hat{u}^+| \to 0$, $|\hat{u}^-| \to 0$ as $\alpha > 0$, $t \to \infty$, which is indicative of the wave absorbing behavior.

4. Spatial modulation of wave amplitude in finite active system

In order to study the effect of η on the waves in finite rod, let us consider a finite rod element of length L with nodal displacements $\hat{u}(0,\omega_n)$ and $\hat{u}(L,\omega_n)$ and the nodal forces $\hat{f}(0,\omega_n$ and $\hat{f}(L,\omega_n)$. The longitudinal displacement at any cross-section $0 \leqslant x \leqslant L$ can be expressed as

$$\hat{u}(x,\omega_n) = [s]\begin{Bmatrix}\hat{f}(0,\omega_n)\\ \hat{f}(L,\omega_n)\end{Bmatrix}, \tag{39}$$

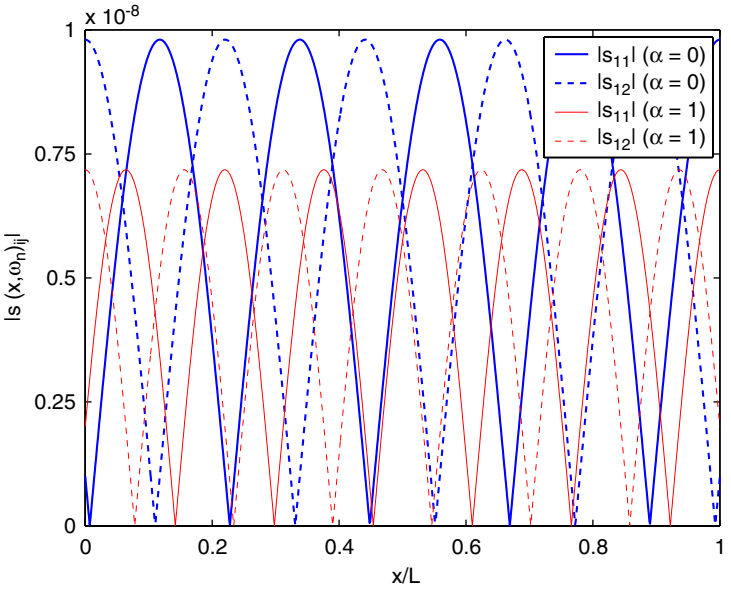

Fig. 3. Frequency response function $[s]$ at various x/L in a finite rod, $\omega_n/2\pi = 10\,\text{kHz}$.

where

$$[s] = \mathrm{i}[\,\mathrm{e}^{-\mathrm{i}k_1 x} \quad \mathrm{e}^{-\mathrm{i}k_2 x}\,] \begin{bmatrix} (A_{11}k_1 + \frac{1}{2}\eta A\omega_n) & (A_{11}k_2 + \frac{1}{2}\eta A\omega_n) \\ -(A_{11}k_1 + \frac{1}{2}\eta A\omega_n)\mathrm{e}^{-\mathrm{i}k_1 L} & -(A_{11}k_2 + \frac{1}{2}\eta A\omega_n)\mathrm{e}^{-\mathrm{i}k_2 L} \end{bmatrix}^{-1}. \tag{40}$$

Under unit impulse excitation, s_{11} and s_{12} are the frequency response functions for longitudinal displacements at x. Fig. 3 shows the reduction in the amplitude of the frequency response and shifts in the phases due to $\alpha = 1$ over x/L at a 10 kHz frequency.

5. Single-sensor non-collocated feedback

In order to introduce the damping mechanism in the active system, let us first consider a single sensor for non-collocated feedback in a rod segment shown in Fig. 4. The design objective here is to obtain the range of admissible η and subsequently the controller transfer functions for a given sensor location x_s. If an equivalently damped system is assumed to achieve this, the dynamic equilibrium equation (see [12]) for the rod segment can be written as

$$[\hat{K}] \begin{Bmatrix} \hat{u}(0,\omega_n) \\ \hat{u}(L,\omega_n) \end{Bmatrix} = \begin{Bmatrix} \hat{f}(0,\omega_n) \\ \hat{f}(L,\omega_n) \end{Bmatrix}, \tag{41}$$

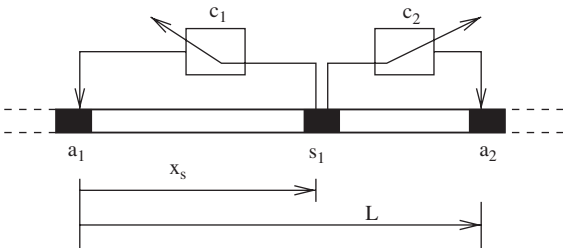

Fig. 4. Single sensor PID feedback wave controller configuration in rod segment of length L. s_1 is the sensor connected to the two controller c_1 and c_2, a_1 and a_2 are the two compliant actuators.

where

$$[\hat{K}] = \frac{\mathrm{i}}{\mathrm{e}^{-\mathrm{i}k_2L} - \mathrm{e}^{-\mathrm{i}k_1L}} \times \begin{bmatrix} (A_{11}k_1 + \frac{1}{2}\eta A\omega_n) & (A_{11}k_2 + \frac{1}{2}\eta A\omega_n) \\ -(A_{11}k_1 + \frac{1}{2}\eta A\omega_n)\mathrm{e}^{-\mathrm{i}k_1L} & -(A_{11}k_2 + \frac{1}{2}\eta A\omega_n)\mathrm{e}^{-\mathrm{i}k_2L} \end{bmatrix} \begin{bmatrix} \mathrm{e}^{-\mathrm{i}k_2L} & -1 \\ -\mathrm{e}^{-\mathrm{i}k_1L} & 1 \end{bmatrix}. \tag{42}$$

A representative volume element in the active system can be designed using this dynamic equilibrium as reference, if the two feedback controllers shown in Fig. 4 have the transfer functions $\hat{c}_1$ and $\hat{c}_2$, such that

$$[\hat{K}_0]\begin{Bmatrix} \hat{u}(0,\omega_n) \\ \hat{u}(L,\omega_n) \end{Bmatrix} - \begin{Bmatrix} \hat{c}_1(\omega_n) \\ \hat{c}_2(\omega_n) \end{Bmatrix}\hat{u}_s = \begin{Bmatrix} \hat{f}(0,\omega_n) \\ \hat{f}(L,\omega_n) \end{Bmatrix}, \tag{43}$$

where $[\hat{K}_0]$ is the dynamic stiffness matrix for the nominal system ($\eta = 0$), $\hat{u}_s$ is the longitudinal displacement at x_s measured by the sensor. The controllers can be designed to perform as linear PID controller, with their output or the actuation forces given by

$$\begin{aligned} \hat{y}_j &= \hat{c}_j\hat{u}_s \\ &= [\hat{c}_{1j}(\mathrm{i}\omega_n)\mathrm{e}^{\mathrm{i}\omega_n\Delta t_1} + \hat{c}_{2j}\mathrm{e}^{\mathrm{i}\omega_n\Delta t_2} + \hat{c}_{3j}(\mathrm{i}\omega_n)^2\mathrm{e}^{\mathrm{i}\omega_n\Delta t_3}]\hat{u}_s, \quad j = 1,2, \end{aligned} \tag{44}$$

where $\hat{c}_{2j}$, $\hat{c}_{2j}$ and $\hat{c}_{3j}$ are, respectively, the transfer functions corresponding to velocity proportional, integral and derivative input. Δt_1, Δt_2 and Δt_3 are, respectively, the time delays associated with these linear input. The longitudinal displacement at the sensor location can further be expressed in terms of the boundary nodal displacements as

$$\hat{u}_s = \frac{1}{\sin(k_0L)}[\sin(k_0(L - x_s)) \quad \sin(k_0x_s)]\begin{Bmatrix} \hat{u}(0,\omega_n) \\ \hat{u}(L,\omega_m) \end{Bmatrix}. \tag{45}$$

The final step is now to equate Eqs. (42) and (43) and find the conditions for the sensor placement (x_s) and the range of admissible solution in $\hat{c}_1$ and $\hat{c}_2$ as functions of (η, x_s). Equating the (1, 1) and (1, 2) components of the matrices on the left hand side of Eqs. (41) and (43) separately, and

combining them into one equation by eliminating $\hat{c_1}$, and then equating the real parts, we get,

$$\frac{\sin(k_0 x_s)}{\sin(k_0(L-x_s))} = \frac{-\dfrac{k_0}{\sin(k_0 L)} + \dfrac{(k_1-k_2)[\sin(k_1 L)-\sin(k_2 L)]}{2[1-\cos((k_1-k_2)L)]}}{k_0\dfrac{\cos(k_0 L)}{\sin(k_0 L)} - \dfrac{(k_1-k_2)\sin((k_1-k_2)L)}{2[1-\cos((k_1-k_2)L)]}} \tag{46}$$

and equating the imaginary parts, we get,

$$\frac{\sin(k_0 x_s)}{\sin(k_0(L-x_s))} = -\frac{A_{11}(k_1-k_2)[\cos(k_2 L)-\cos(k_1 L)]}{A_{11}\psi_1 + \frac{1}{2}\eta A \omega_n \psi_2}, \tag{47}$$

where

$$\begin{aligned}\psi_1 &= [k_1\cos(k_2 L) - k_2\cos(k_1 L)][\cos(k_2 L)-\cos(k_1 L)]\\ &\quad -[k_1\sin(k_2 L) - k_2\sin(k_1 L)][\sin(k_1 L)-\sin(k_2 L)],\\ \psi_2 &= [\cos(k_2 L)-\cos(k_1 L)]^2 + [\sin(k_1 L)-\sin(k_2 L)]^2.\end{aligned}$$

Similarly, by equating (2, 1) and (2, 2) components of the matrices on the left-hand side of Eqs. (41) and (43) separately, and following the same procedure as earlier by eliminating $\hat{c_2}$, the real parts yield

$$\frac{\sin(k_0 x_s)}{\sin(k_0(L-x_s))} = \frac{\dfrac{k_0\cos(k_0 L)}{\sin(k_0 L)} - \dfrac{\psi_3}{2[1-\cos(k_1-k_2)L]}}{-\dfrac{k_0}{\sin(k_0 L)} + \dfrac{\psi_4}{2[1-\cos(k_1-k_2)L]}}, \tag{48}$$

where

$$\begin{aligned}\psi_3 &= [k_1\cos(k_1 L) - k_2\cos(k_2 L)][\sin(k_1 L)-\sin(k_2 L)]\\ &\quad -[k_2\sin(k_2 L) - k_1\sin(k_1 L)][\cos(k_2 L)-\cos(k_1 L)],\\ \psi_4 &= (k_1-k_2)\cos((k_1+k_2)L)[\sin(k_1 l)-\sin(k_2 L)]\\ &\quad +(k_1-k_2)\sin((k_1+k_2)L)[\cos(k_2 L)-\cos(k_1 L)],\end{aligned}$$

and the imaginary parts yield

$$\frac{\sin(k_0 x_s)}{\sin(k_0(L-x_s))} = \frac{-A_{11}\dfrac{\psi_5}{[1-\cos((k_1-k_2)L)]} + \eta\omega_n}{A_{11}\dfrac{\psi_6}{[1-\cos((k_1-k_2)L)]}}, \tag{49}$$

where

$$\begin{aligned}\psi_5 &= [k_1\cos(k_1 L) - k_2\cos(k_2 L)][\cos(k_2 L)-\cos(k_1 L)]\\ &\quad +[k_2\sin(k_2 L) - k_1\sin(k_1 L)][\sin(k_1 L)-\sin(k_2 L)],\\ \psi_6 &= (k_1-k_2)\cos((k_1+k_2)L)[\cos(k_2 L)-\cos(k_1 L)]\\ &\quad -(k_1-k_2)\sin((k_1+k_2)L)[\sin(k_1 L)-\sin(k_2 K)].\end{aligned}$$

The common solution from Eqs. (47) and (49) is

$$\cos(k_1 L) = \cos(k_2 L) \Rightarrow \eta = \sqrt{\frac{4\pi^2 m^2 A_{11}^2}{\omega_n^2 L^2 A^2} - \frac{4A_{11}I_0}{A^2}}, \quad m = 1, 2, \ldots \tag{50}$$

such that η is real and positive. The common solution from Eqs. (46) and (48) is

$$\frac{2k_0}{k_1 - k_2} = \left[\frac{\sin(k_0 L)}{1 + \cos(k_0 L)}\right]\left[\frac{\sin(k_1 L) - \sin(k_2 L) + \sin((k_1 - k_2)L)}{1 - \cos((k_1 - k_2)L)}\right]. \tag{51}$$

Imposing the solution from Eq. (50) in Eq. (51), one can write

$$\sin((k_1 - k_2)L) = 0 \Rightarrow \eta = \sqrt{\frac{\pi^2 l^2 A_{11}^2}{\omega_n^2 L^2 A^2} - \frac{4A_{11}I_0}{A^2}}, \quad l = 1, 2, \ldots \tag{52}$$

such that η is real and positive, which is an essential condition for guaranteed stability and wave absorbing properties. This implies the common solution for $l = 2m$. Fig. 5 shows the admissible solution space in η to achieve this exact dynamics artificially introduced through the feedback controllers. The figure also shows the range of wavelengths $\lambda_1 = 2\pi/k_1$ and $\lambda_2 = 2\pi/k_2$ at which such dynamics can be introduced. The figure also shows that for a specified set of η, a set of discrete values of forward and backward propagating waves can be controlled exactly.

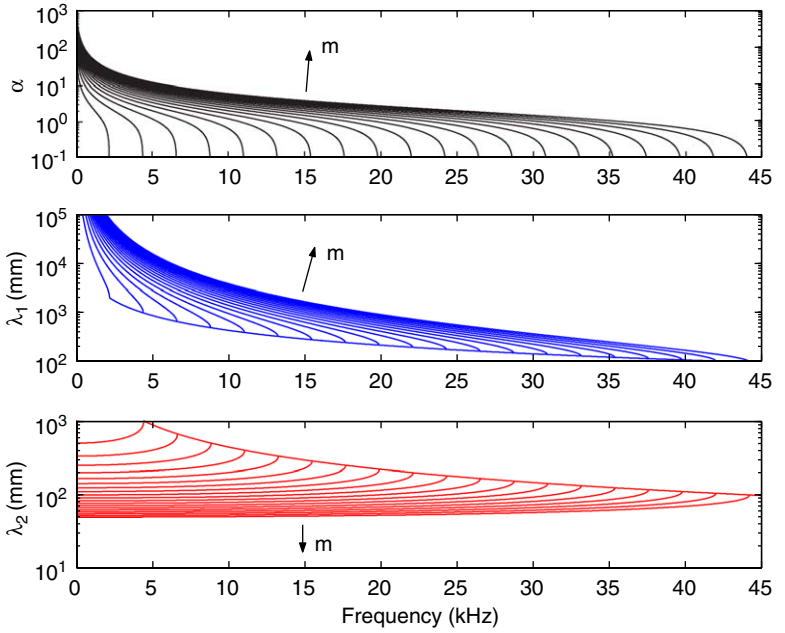

Fig. 5. Solution space for single sensor feedback for an arbitrary sensor location x_s. $\alpha = \eta^2/(4\rho E)$. The arrows indicate the growth of the envelops for increasing m in Eq. (50).

With the help of Eqs. (46)–(49), the transfer function of the two controllers can be written as

$$\hat{c}_1 = \frac{1}{\sin(k_0(L-x_s))}\,\hat{G}_1(\eta,\omega_n), \quad \hat{c}_2 = \frac{1}{\sin(k_0 x_s)}\,\hat{G}_2(\eta,\omega_n), \tag{53}$$

where

$$\hat{G}_1(\eta,\omega_n) = \frac{1}{(e^{-ik_2L}-e^{-ik_1L})}\Bigg[-iA_{11}\sin(k_0L)(k_1e^{-ik_2L}-k_2e^{-ik_1L}) + i\left\{A_{11}k_0\cos(k_0L)-\frac{1}{2}\eta A\omega_n\sin(k_0L)\right\}(e^{-ik_2L}-e^{-ik_1L})\Bigg], \tag{54}$$

$$\hat{G}_2(\eta,\omega_n) = \frac{1}{(e^{-ik_2L}-e^{-ik_1L})}\Bigg[-iA_{11}\sin(k_0L)(k_1e^{-ik_1L}-k_2e^{-ik_2L}) + i\left\{A_{11}k_0\cos(k_0L)+\frac{1}{2}\eta A\omega_n\sin(k_0L)\right)(e^{-ik_2L}-e^{-ik_1L}\Bigg\}\Bigg]. \tag{55}$$

5.1. Controller characteristics

Eqs. (54) and (55) show that for a sensor location x_s, the poles of the transfer functions are at

$$\sin(k_0(L-x_s)) = 0 \quad \Rightarrow \quad \frac{x_s}{L} = 1-\left(\frac{p}{2}\right)\frac{\lambda_0}{L}, \quad p = 0,1,2,\ldots \tag{56}$$

and

$$\sin(k_0x_s) = 0 \quad \Rightarrow \quad \frac{x_s}{L} = \left(\frac{q}{2}\right)\frac{\lambda_0}{L}, \quad q = 0,1,2,\ldots, \tag{57}$$

where $\lambda_0 = 2\pi/k_0$ is the wavelength in the nominal system. Fig. 6 shows the distribution of the transfer function poles over the frequency axis, depending upon the sensor location (x_s/L) governed by Eqs. (56) and (57).

It can be seen in Eqs. (54) and (55) that the other poles of the transfer functions, which are dependent on η, satisfy the condition

$$e^{-ik_2L}-e^{-ik_1L} = 0, \tag{58}$$

which leads to Eqs. (50) and (52). Distribution of these poles over the frequency axis for a given η is the horizontal cut on the branches of α plotted in Fig. 5. This indicates that at higher values of the damping, the desired controllers will have more number of their poles concentrated at low-frequency region. By studying the numerators of $\hat{G}_1$ and $\hat{G}_2$, it can be observed that the zeros of the transfer functions lie at $\eta = 0$. Hence they do not have any influence on the controller sensitivity. Figs. 7–10 show the amplitude and phase of the two transfer functions for various target α. It can be seen that for both the controllers, the poles, which are governed by the damping coefficient η, should be placed identically over the frequency axis. Between the two transfer functions, an anti-symmetric phase behavior with respect to each of the poles can be noted. This is irrespective of the values of the target η. It can also be seen from these figures that more number of

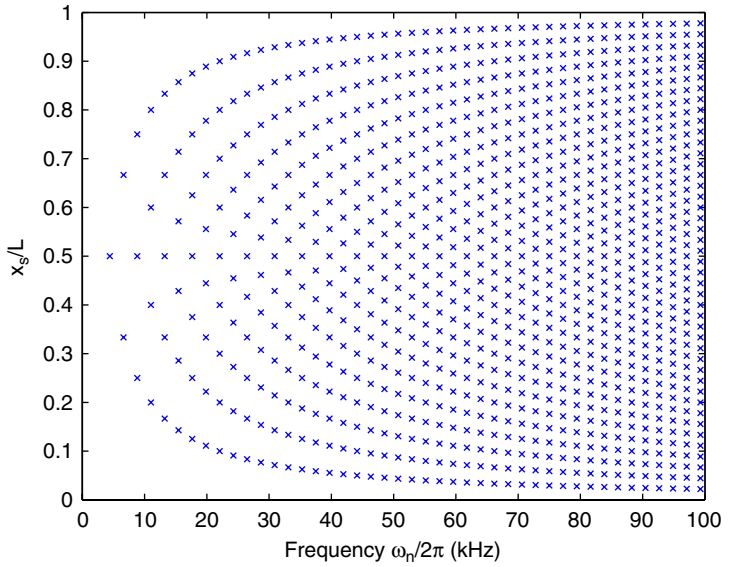

Fig. 6. Poles of the controller transfer functions over frequency axis for various sensor locations (x_s/L).

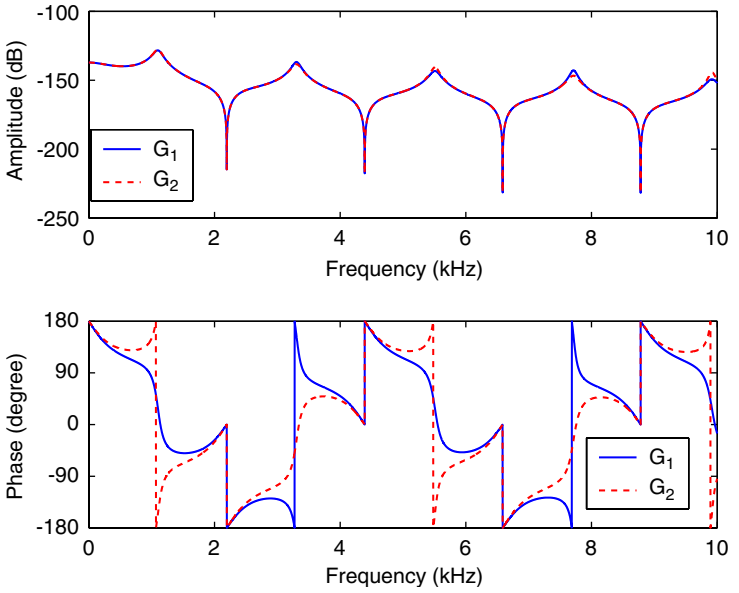

Fig. 7. Amplitude and phase of the controller transfer functions for target $\alpha = 0.01$.

poles move in toward the lower frequencies for higher damping. However, for broadband applications involving shock-type loading on the material system, these may create additional disturbances outside the target range of frequencies. Therefore, in such situations, a band-pass-type filter may be required to augment the controller design.

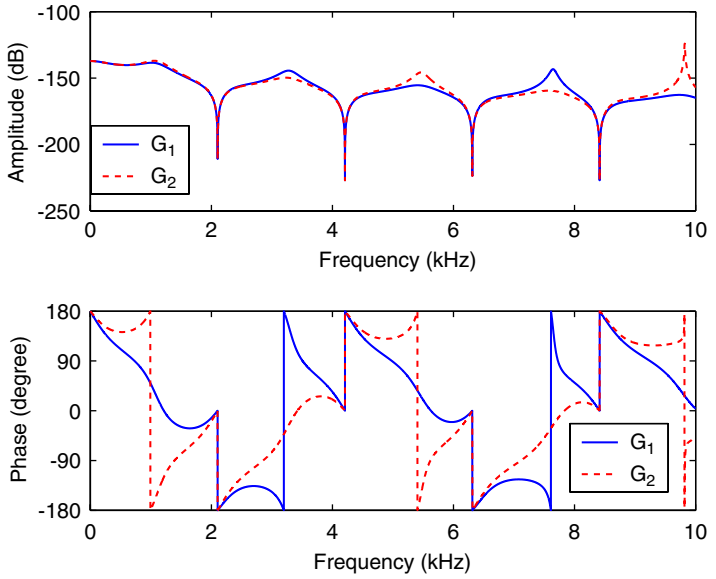

Fig. 8. Amplitude and phase of the controller transfer functions for target $\alpha = 0.1$.

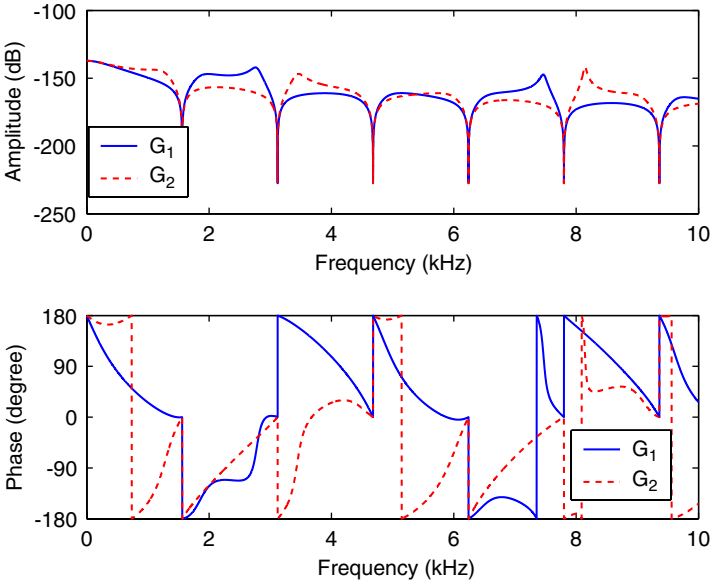

Fig. 9. Amplitude and phase of the controller transfer functions for target $\alpha = 1$.

6. Conclusions

Two types of material system, namely the passive system and the active system, are considered in this paper to study their equivalence in terms of wave control performance. The passive

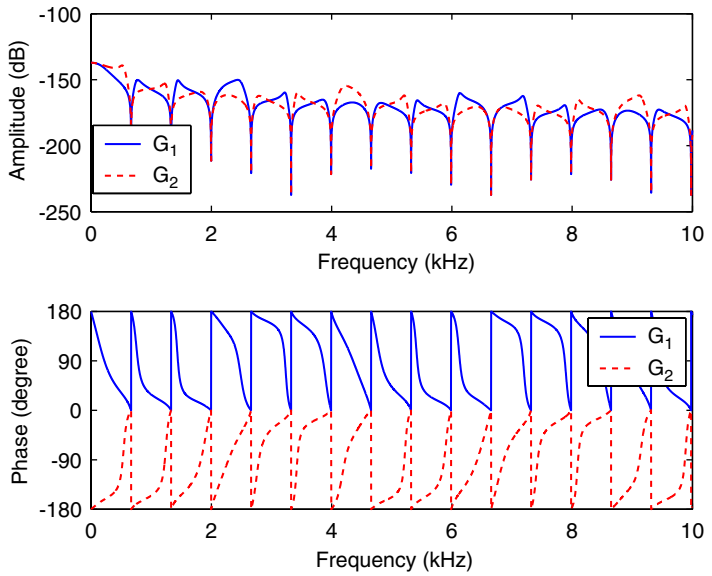

Fig. 10. Amplitude and phase of the controller transfer functions for target $\alpha = 10$.

material system, which has stress relaxation property, shows asymmetry of the wave dispersion with respect to the half-line ($x = 0$). Although non-dispersive, the forward propagation is faster compared to the backward propagation in such system. In order to introduce the corresponding damping mechanism in the active material system with array of active transducers and feedback controllers, a systematic design methodology is proposed. The power flow and the asymptotic stability of such equivalent system are discussed. The results show that unconditional stability can be achieved if appropriate boundary control mechanism is designed. The exact solution space in terms of the target damping coefficient and target wavelengths is obtained. The characteristics of the feedback controller transfer functions is discussed by considering the placement of the sensor and variation in the target damping coefficient. Similar design methodology may be employed for other types of dispersive and dissipative material systems involving more complex constitutive property of the passive material and array of micro-electro-mechanical transducers and microcontrollers.

Acknowledgements

The author gratefully acknowledges the support from the AR&DB Center for Composite Structures at the Department of Aerospace Engineering during this work and fruitful discussion with Dr. S. Gopalakrishnan.

References

[1] H. Fujii, T. Ohtsuka, T. Murayama, Wave-absorbing control for flexible structures with noncollocated sensors and actuators, *Journal of Guidance, Control and Dynamics* 15 (2) (1992) 431–439.

[2] S.J. Elliott, L. Billet, Adaptive control of flexural wave propagating in a beam, *Journal of Sound and Vibration* 163 (2) (1993) 295–310.
[3] S.-Y. Lee, C.D.Jr. Mote, Wave characteristics and vibration control of translating beams by optimal boundary damping, *ASME Journal of Vibration and Acoustics* 121 (1999) 18–25.
[4] N. Tanaka, Y. Kikushima, Optimal vibration feedback control of an Euler–Bernoulli beam: toward realization of the active sink method, *ASME Journal of Vibration and Acoustics* 121 (1999) 174–182.
[5] H. Alli, T. Singh, On the feedback control of the wave equation, *Journal of Sound and Vibration* 234 (4) (2000) 625–640.
[6] A. Yousefi-Koma, G. Vukovich, Vibration suppression of flexible beams with bonded piezotransducers using wave-absorbing controllers, *Journal of Guidance, Control and Dynamics* 23 (2) (2000) 347–354.
[7] A. Baz, Spectral finite-element modeling of the longitudinal wave propagation in rods treated with active constrained layer damping, *Smart Materials and Structures* 9 (2000) 372–377.
[8] J.N. Aubrun, Theory of the control of structures by low authority controllers, *Journal of Guidance, Control and Dynamics* 3 (5) (1980) 444–451.
[9] D.B. Schaechter, Optimal local control of flexible structures, *Journal of Guidance, Control and Dynamics* 4 (1) (1981) 22–26.
[10] G.S. Nurre, R.S. Ryan, H.N. Scofield, J.L. Sims, Dynamics and control of large space structures, *Journal of Guidance, Control and Dynamics* 7 (5) (1984) 514–526.
[11] O. Thorp, M. Ruzzene, A. Baz, Attenuation and localization of wave propagation in rods with periodic shunted piezoelectric patches, *Smart Materials and Structures* 10 (2001) 979–989.
[12] D. Roy Mahapatra, S. Gopalakrishnan, B. Balachandran, Active feedback control of multiple waves in helicopter gearbox support struts, *Smart Materials and Structures* 10 (2001) 1046–1058.
[13] C.H. Chung, C.A. Tan, Active vibration control of the axially moving string by wave cancellation, *ASME Journal of Vibration and Acoustics* 117 (1995) 49–55.
[14] D.W. Miller, S.R. Hall, A.H. von Flotow, Optimal control of power flow at structural junctions, *Journal of Sound and Vibration* 140 (3) (1990) 475–497.
[15] P. Gardonio, S.J. Elliott, Active control of waves on a one-dimensional structure with a scattering terminations, *Journal of Sound and Vibration* 192 (3) (1996) 701–730.
[16] S. Gopalakrishnan, D. Roy Mahapatra, Optimal spectral control of broadband waves in smart composite beams with distributed sensor-actuator configuration, *SPIE Symposium on Smart Materials and MEMS*, Melbourne, Australia, December 13–15, Paper No. 4234-12, 2000.
[17] J.L. Fanson, T.K. Caughey, Positive position feedback control for large space structures, *AIAA Journal* 28 (4) (1990) 717–724.
[18] S.K. Burke, J.K.J. Hubbard, J.K. Meyer, Colocation: design constraints for distributed and discrete transducers, *Proceedings of the 13th Biennial Conference on Mechanical Vibration and Noise*, DE vol. 34, Miami, FL, September 22–25, 1991, pp. 75–81.
[19] A.H. von Flotow, The acoustic limit of control of structural dynamics, in: S.N. Atluri, A.K. Amos (Eds.), *Large Space Structures: Dynamics and Control*, Springer, Berlin, 1988, pp. 213–237.
[20] V. Krylov, S.V. Sorokin, Dynamics of elastic beams with controlled distributed stiffness parameters, *Smart Materials and Structures* 6 (1997) 573–582.
[21] S.V. Sorokin, O.A. Ershova, S.V. Grishina, The active control of vibrations of composite beams by parametric stiffness modulation, *European Journal of Mechanics of Solids A* 19 (2000) 873–890.
[22] K.A. Lurie, Effective properties of smart elastic laminates and the screening phenomenon, *International Journal of Solids and Structures* 34 (13) (1997) 1633–1643.
[23] G.W. Milton, *The Theory of Composites*, Cambridge University Press, Cambridge, 2002.
[24] S. Acharjee, N. Zabaras, A proper orthogonal decomposition approach to microstructure model reduction in Rodrigues space with application to optimal control of microstructure-sensitive properties, *Acta Materialia* 51 (2003) 5627–5646.
[25] P.W. Chung, R.R. Namburu, On a formulation for a multiscale atomistic homogenization method, *International Journal of Solids and Structures* 40 (2003) 2563–2588.